

Forest change detection by statistical object-based method

Baudouin Desclée, Patrick Bogaert, Pierre Defourny*

Department of Environmental and Land Use Planning, Université Catholique de Louvain, Place Croix du Sud, 2 bte 16, B-1348 Louvain-la-Neuve, Belgium

Received 20 June 2005; received in revised form 13 January 2006; accepted 15 January 2006

Abstract

Forest monitoring requires more automated systems to analyse the large amount of remote sensing data. A new method of change detection is proposed for identifying forest land cover change using high spatial resolution satellite images. Combining the advantages of image segmentation, image differencing and stochastic analysis of the multispectral signal, this OB-Reflectance method is object-based and statistically driven. From a multivariate image, a single segmentation using region-merging technique delineates multivariate objects characterised by their reflectance differences statistics. Objects considered as outliers from multitemporal point of view are successfully discriminated thanks to a statistical procedure, i.e., the iterative trimming. Based on a chi-square test of hypothesis, abnormal values of reflectance differences statistics are identified and the corresponding objects are labelled as change. The object-based method performances were assessed using two sources of reference data, including one independent forest inventory, and were compared to a pixel-based method using the RGB-NDVI technique. High detection accuracy (>90%) and overall Kappa (>0.80) were achieved by OB-Reflectance method in temperate forests using three SPOT-HRV images covering a 10-year period.

© 2006 Elsevier Inc. All rights reserved.

Keywords: Change detection; Forest; Image segmentation; Multivariate; Satellite images

1. Introduction

Forest ecosystems have never been so affected by human pressure than currently (FAO, 2001). The rapid conversion or degradation of forest environments is thus of important international concern. Forest monitoring mainly focuses on detecting and estimating the land conversion rate and, more recently, on assessing carbon stocks in the forest ecosystem. Operational systems for monitoring and updating forest maps are thus needed for many applications such as forest management, carbon budgeting and habitat monitoring (de Wasseige & Defourny, 2004; Foody, 2003; Sader et al., 2001).

Satellite remote sensing is widely used to detect forest change and update existing forest maps. Many change detection techniques have been developed since the early days of earth observation. They can be broadly grouped into three categories: (1) visual interpretation, (2) pixel-based methods and (3) object-based approaches.

Visual interpretation using single or multivariate images requires human expertise (computer-assisted or not) for delimiting and labelling zones that are considered as changed. This method can make full use of an analyst's experience and knowledge. Texture, shape, size and patterns of the images are key elements for identification of land cover change through visual interpretation (Lu et al., 2004). Although this technique is time-consuming and requires skilled analysts, visual interpretation is still widely used (Asner et al., 2002; Sunar, 1998). Currently, there is no automatic image processing able to grasp the high complexity of land cover changes made by the combination of several factors such as the stage or the size of the change area. That is why change maps produced for large-area projects with many land cover changes classes like CORINE Land Cover 2000 (Büttner et al., 2002) or Forest Resources Assessment (FAO, 2001) were still based on this technique.

Digital pixel-based change detection methods provide more quantitative and repeatable information compared to visual interpretation. Several authors (Coppin & Bauer, 1996; Lu et al., 2004) have reviewed pixel-based methods but theirs

* Corresponding author. Fax: +32 10478898.

E-mail address: defourny@enge.ucl.ac.be (P. Defourny).

performances are rarely compared to each other. In this category of techniques, the multidate classification or composite analysis that deals with different satellite images in one aggregated analysis is known to be straightforward (Hall et al., 1984). As a single classification is performed in one step, it avoids combining respective inaccuracies that are common with postclassification comparison procedures. Sader et al. (2001) have stacked the NDVI of 3 dates in a red, green and blue composite to perform an unsupervised classification. This specific multidate classification denoted as RGB-NDVI avoids the need of setting a predefined histogram threshold, but it requires training sample data to label classes. Hayes and Sader (2001) found the RGB-NDVI method to be more accurate than NDVI image differencing and principal component analysis. Despite their good change detection accuracy, many of these techniques are considered scene-dependent (Lyon et al., 1998; Rogan et al., 2003). The thresholding step or classification process developed from one set of images cannot be directly applied to other regions with other satellite data. Moreover, more complex procedures combining several methods have also been proposed but they become dedicated to specific changes such as urban expansion, conifer mortality and transitions from tundra to boreal forest (Li & Yeh, 1998; Macomber & Woodcock, 1994; Silapaswan et al., 2001). Finally, the main drawback of pixel-based methods is the “salt and pepper” effect in the resulting maps. This is due to the random variation of the sensor’s response, but also to an intrinsic characteristic of the land cover element itself (Lobo, 1997). Indeed, the useful spatial, or contextual, information between the values of proximate pixels is most often ignored (Atkinson & Lewis, 2000; Townshend et al., 2000).

More recently, object-based methods have been proposed for forest change detection to combine the contextual analysis of visual interpretation with the quantitative aspect of pixel-based approaches. Instead of analysing pixels independently of their location, similar contiguous pixels are grouped into objects. Initially, object boundaries specified by forest stand delineation vectors were derived from a Geographic Information System (GIS) (Coppin & Bauer, 1995; Heikkonen & Varjo, 2004; Kayitakire et al., 2002; Varjo, 1996; Walter, 2004; Wulder et al., 2004). The interest for object-based methods has increased with the improvements in image segmentation techniques (Flanders et al., 2003; Mäkelä & Pekkarinen, 2001). Image segmentation is the division of the satellite image into spatially continuous and homogeneous regions, hereafter named as objects. The main advantage of object-based methods is the incorporation of contextual information in the change analysis (Flanders et al., 2003). Moreover, the segmentation reduces the local spectral variation inducing better discrimination between land cover types (Lobo, 1997). However, although the object delineation remains crucial, a limitation is the definition of a Minimum Mapping Unit (MMU). Defined initially to control the visual interpretation process (Saura, 2002), this parameter defines the minimum size of an object as calculated by its number of included pixels (Mäkelä & Pekkarinen, 2001). So, change areas smaller than this constraint could not be detected by the change analysis.

Because of the enormous amount of remote sensing data to analyse, operational monitoring systems require more automated methods. An efficient change detection procedure should be objective, easy to use, and should require a limited number of parameters for extracting changes. Indeed, the huge amount of work that has been done in change-thresholding of the histograms of vegetation-difference-images clearly warrants the reduction of human intervention in the process (Bruzzone & Prieto, 2000; Fung & LeDrew, 1988; Jin & Sader, 2005; Le Hégarat-Masclé & Seltz, 2004). By using an automated procedure, this time-consuming human interpretation could thus be limited to the class labelling of the identified changed areas. However, in spite of increasing demand connected with international concern about forests, very few automatic algorithms have been proposed in the literature (Rogan & Chen, 2004). Taking advantages of object-based techniques, two methods have already been developed but they suffered of low detection performances. The first one is the unsupervised technique of Häme et al. (1998) which is based on change vector analysis. By analysing groups of pixels to reduce the “salt and pepper” effect, this technique does not take advantage of image segmentation. The second one is based on a presegmentation step coupled with an unsupervised ISODATA classification (Saksa et al., 2003). This technique failed to correctly extract clear-cut areas because the segmentation and the clustering algorithm were not appropriate (MMU too large and classification based on object difference means).

This research aims to develop a new method to extract land cover changes in forest by taking advantages of image segmentation, image differencing and stochastic analysis of the multispectral signal. Using high spatial resolution images, this method was sought to be scene-independent and easy-to-use. This study also aims to test this new approach on a multi-year SPOT-HRV data set and to compare its performances to the pixel-based method using the RGB-NDVI technique.

2. Study site and data

The study site covers more than 1800 km² and is located in Eastern Belgium. The forests that cover 40% of the total area include both deciduous and coniferous stands, with the last type being dominant. Land cover changes are more frequent and cover larger areas in conifer stands because they are rather monospecific and have a shorter exploitable age. Whereas different forest management systems coexist, many clear cuttings occurred in coniferous stands on areas ranging from 0.1 to more than 10 ha. After clear-cuttings, the forest regeneration can either rely on natural recolonisation or young tree plantation. The distinction between these two regeneration techniques is not possible using SPOT-HRV data.

Three cloud-free multispectral SPOT-HRV images were acquired over a decade and are considered as our multidate data set. Near-anniversary dates during the phenological peak season were selected in order to reduce the seasonality effect. The acquisition dates for these images were August 7th 1992 (XS92), July 24th 1995 (XS95) and September 14th 2003 (XS03), respectively from SPOT-2, -3 and -5 satellites. The

difference in the spatial resolution between images (20m for the first two and 10m for the last one) was corrected by bilinear interpolation resampling of the last image (XS03) to 20 m. Moreover, because the ShortWave InfraRed band was only available for the last acquisition, this spectral band was not used in the study. The 3 spectral bands, respectively Green (G), Red (R) and Near-Infrared (NIR), were combined for the 3 dates in a 9-band multivariate data set.

Ancillary data included a forest inventory data layer, GIS topomaps, aerial photographs, the 1990 CORINE Land Cover (CLC) map and a Digital Elevation Model (DEM). The 2003 updated forest inventory of the state-owned forest was provided in GIS vector format including stand properties, such as the species composition and the date of the last planting. Forest stands were delineated from aerial photographs with a MMU of less than 0.1 ha and stand characteristics were collected on the field. This independent data source was used as reference for the accuracy assessment. Topographic maps of 1:10,000 scale were used for the field survey. A set of digital and orthorectified aerial photographs of 1:20,000 scale acquired in 1997–1998 was also available for the selection of very precise ground control points (GCP) for accurate coregistration and validation. The CLC map, as produced by classification of Landsat images in 1990, served as a coarse independent forest mask which was then visually improved. Finally, a 30m DEM was resampled at 20m by bilinear interpolation for the orthorectification of the satellite images.

Two preprocessing steps were required for a meaningful comparison of the satellite images. First, a coregistration between the three images was carried out with high precision to avoid misregistration errors inducing false change alerts. Depending on the satellite image, a set of 18 to 26 GCPs spread over the whole study area were selected from aerial photographs. Orthorectification using the DEM was then applied on each image. The Root Mean Square Errors (RMSE) were respectively 0.51, 0.66 and 0.39 pixels. Secondly, as significant radiometric differences between images (due to geometry of acquisition and sensor calibration) could prevent the comparison of absolute reflectance values in multitemporal analyses (Häme, 1991), the radiance of images was radiometrically corrected into top-of-atmosphere (TOA) reflectance using the calibration parameters of Spotimage (Lillesand & Kiefer, 2000). In order to apply the RGB-NDVI method, the Normalized Difference Vegetation Index (NDVI) was calculated from the TOA reflectance channels (NIR and R) respectively for each image where

$$\text{NDVI} = \frac{(\text{NIR} - \text{R})}{(\text{NIR} + \text{R})} \quad (1)$$

From the 3 satellites images, two multivariate data sets were produced: (i) the 3 NDVI bands, and (ii) the 9 TOA reflectance channels.

3. Object-based methodology

The proposed change detection method is object-based and statistically driven. This technique, presented in Fig. 1, includes

3 steps resulting in the production of change maps. First, the multivariate segmentation partitions the whole multi-year image into objects. Second, the object multivariate signatures are extracted from each object to characterise the object spectro-temporal behaviour. Third, the multivariate iterative trimming is a statistical procedure to identify changed objects based on their object signatures.

Over the time span covered by a sequence of satellite images, the change detection algorithm aims to distinguish “changed objects”, corresponding to areas with (land cover) change, from “unchanged objects” (i.e., regular forest growth stands). The proposed algorithm relies on three basic assumptions: (i) changes are rare and concern a small part of the total study area, (ii) unchanged objects exhibit similar reflectance differences and (iii) changes induce large surface reflectance variation and abnormal reflectance differences. Assuming these hypotheses hold, the algorithm measures for each object the surface reflectance variation over time and compares it between objects. Object exhibiting abnormal reflectance change over time can thus be statistically identified and labelled as changed areas. It is worth noting that the proposed basic assumptions are most often respected for forested areas, even if the change proportion clearly depends on the time interval between observations as well as on the region size. As a confirmation of the second assumption, Liang et al. (1997) and Coppin and Bauer (1994) take advantage of unchanged forests as stable targets for radiometric calibration between multivariate images.

3.1. Multivariate segmentation

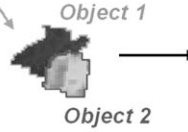
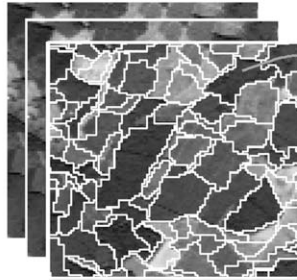
Image segmentation is the process of partitioning an image into groups of pixels that are spectrally similar and spatially adjacent, by minimizing the within-object variability compared to the between-object variability. The object delineation has been achieved here using a general segmentation algorithm based on homogeneity definitions, in combination with local and global optimisation techniques, as implemented in the e-Cognition commercial software (Baatz & Schäpe, 2000). The segmentation algorithm is a region-merging technique which fuses the objects according to an optimisation function given by Eq. (2), with

$$w_{\text{spectral}} \sum_{\text{nb}} w_b \sigma_b + (1 - w_{\text{sp}}) \left(w_{\text{cp}} \frac{l}{\sqrt{\text{np}}} + (1 - w_{\text{cp}}) \frac{l}{\text{lr}} \right) \leq h_{\text{sc}} \quad (2)$$

where nb is the number of spectral bands, σ_b is the within-object variance for the spectral band b , l is the object border length, np is the number of pixels and lr is the shortest possible length given the rectangle bounding the pixels (although each band b can potentially have a specific weight, referred to as w_b , the same weight has been considered for all bands in this study). This function also includes three kinds of user-defined parameters or weights. The spectral parameter w_{sp} , trading spectral homogeneity vs. object shape, is included in order to

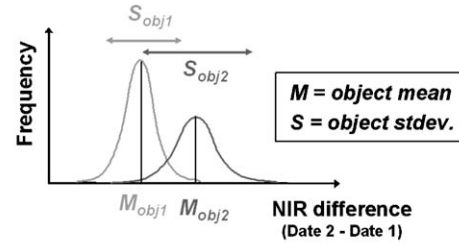
1. Multidate segmentation

One single image segmentation on the multidate image



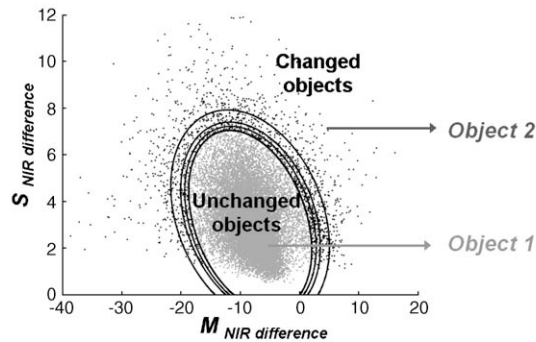
2. Object multidate signature

Two object-statistics (M & S) derived from the reflectance difference bands



3. Multivariate iterative trimming

Statistical test to identify changed objects



4. Change map

Hatched regions = change

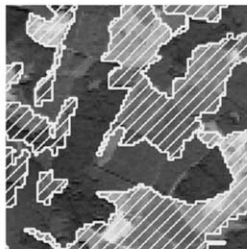


Fig. 1. General principles of the object-based change detection method (OB-Reflectance).

obtain spectrally homogenous objects while irregular or branched objects are avoided. The compactness parameter w_{cp} , trading compactness vs. smoothness, adjusts the object shape between compact objects and smooth boundaries. Finally, corresponding to the threshold of heterogeneity, the scale parameter h_{sc} controlling the object size has been selected in order that the minimum object size match to the Minimum Mapping Unit (MMU).

Traditionally, the segmentation process has only been applied to one single satellite image (Flanders et al., 2003; Mäkelä & Pekkarinen, 2001; Wulder et al., 2004). In this study, objects are defined in a single operation from the whole set of spectral bands using all sequential images together. This approach, hereafter denoted as multidate segmentation, relies on spatial, spectral and temporal information to delineate suitable objects, so that pixels that are spectro-temporally similar in a nb -dimensional space are grouped together, where nb refers to the number of different spectral bands for the set of sequential images.

3.2. Object multidate signature

In order to compare the multidate evolution of the spectral signal, the reflectance of the three sequential (dates 1, 2 and 3) satellite image was subtracted pair-wise for all pixels belonging to the same object. Thus, two difference images were computed from the successive observations, i.e., dates 2–1 and dates 3–2.

For each object delineated by the previous multidate segmentation, the distribution of the reflectance difference values was summarized by a multidate signature. This signature includes two descriptive statistics, i.e., the mean (M) and the standard deviation (S), corresponding respectively to a measure of surface reflectance difference and heterogeneity. As these differences are computed for each band, the multidate signature X_{ij} of each object can be defined as a vector, with

$$X_{ij} = (M_{ij1}, \dots, M_{ijb}, S_{ij1}, \dots, S_{ijb})' \quad (3)$$

where i refers to the object, j (with $j = 1$ or 2) refers to the image difference considered, and b refers to the number of spectral bands.

3.3. Multivariate iterative trimming

Using the vectors as defined in Eq. (3), changed objects from the unchanged ones were separated by a statistical analysis using an iterative trimming procedure. Trimming is defined as the removal of extreme values that behave like outliers. The common purpose of this procedure is to reduce the sensitivity to outliers for many parameter estimates, such as the sample mean and variance (Kotz et al., 1988). In the case of a Gaussian distribution, the trimmed mean is a robust estimation of the mean that is not affected by outliers. According to Bickel (1965), this estimator is efficient under a variety of

circumstances. More details about this technique can be found in Huber (1972), Hoaglin et al. (1983) and Lee (1995). It is worth noting that the trimming procedure is applied here in a slightly different context. While typically used to eliminate abnormal values, these values need to be kept in our context, as the corresponding objects are classified as changed.

The object reflectance differences over time are similar for undisturbed forests because the local forest heterogeneity is efficiently smoothed out by the combination of image differencing and image segmentation. Assuming that observed differences are due to various uncontrolled factors, the distribution of the multivariate signature parameters for unchanged objects could be reasonably approximated by a Gaussian distribution (this assertion will be validated from the results of the analysis). These limited modifications of the temporal reflectances are also expected to sharply contrast with the high and heterogeneous reflectance modifications in the case of forest change. The statistical values for changed objects thus tend to be located mainly in the head and tail of the distribution, so that they behave like outliers with respect to those for unchanged objects.

In this study, the trimming procedure was performed in its multivariate version, that takes simultaneously into account the different object statistics appearing in each vector X_{ij} . The combination of several variables by way of multivariate analyses strengthened the analysis. Using simultaneously the object standard deviation of reflectance difference in addition to the object mean of reflectance difference for all spectral bands, the capability of detecting changes increases, as e.g., these changes may affect the various spectral bands to different extents. As proposed above, let us assume that for unchanged objects, X_{ij} is Gaussian distributed with mean vector m_j and covariance matrix Σ_j , so that we can define

$$C_{ij} = (X_{ij} - m_j)' \sum_j^{-1} (X_{ij} - m_j) \sim \chi^2(2b) \quad (4)$$

where C_{ij} is chi-square distributed with $2b$ degrees of freedom. We can thus write that

$$P(C_{ij} < \chi_{1-\alpha}^2(2b)) = 1 - \alpha \quad (5)$$

i.e., for a chosen probability level $1 - \alpha$ (with $1 - \alpha = 0.99$, for example), we can identify a value $\chi_{1-\alpha}^2(2b)$ that C_{ij} will only exceed with probability α . If α is chosen to be small, a simple hypothesis test at the $1 - \alpha$ confidence level consists of identifying any C_{ij} value that exceeds this threshold as a potentially outlying value, so that in our context the corresponding object i is flagged as changed. This procedure is similar to the approach applied by Ridd and Liu (1998) using a pixel-based approach, which proved to be efficient to detect changes in an urban environment. The confidence level $1 - \alpha$ can be optimised to the application at hand thanks to a training data set.

Clearly, applying Eq. (4) can only be done if one knows the corresponding m_j and Σ_j . These can be initially estimated

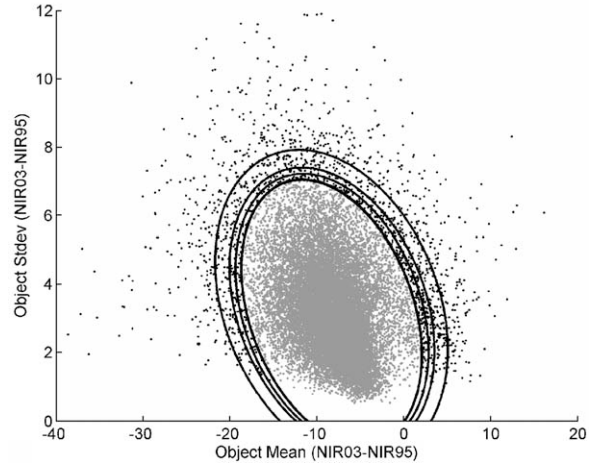


Fig. 2. Detection of changed objects from two statistics describing the reflectance difference (XS03–XS95) for the NIR spectral band, i.e., the mean (Object Mean) and standard deviation (Object Stdev). The iterative process is illustrated by the ellipses drawn for iterations 1, 2, 3 and 13 (out of 13 iterations). Points outside the smallest ellipse (iteration 13) are all considered as changed objects.

directly from the whole set of corresponding X_{ij} vectors, but as this set is precisely expected to contain outlying values, this could lead to poor estimates. We thus propose to use Eqs. (4) and (5) in an iterative approach. Initial estimates \hat{m}_j and $\hat{\Sigma}_j$ are computed from the whole set of objects, and a first trimming is applied. From the set of objects flagged as unchanged, new estimates \hat{m}_j and $\hat{\Sigma}_j$ are obtained, and trimming can be applied again. This iterative procedure is stopped when no new objects are flagged as changed. Instead of extracting changed objects in a single step from poor initial estimates \hat{m}_j and $\hat{\Sigma}_j$, the selection of outliers thus becomes finer at each new iteration. An illustration of the iterative procedure results is given in Fig. 2, where only a single band has been used for the sake of simplicity; as the number of iterations increases, the corresponding confidence ellipses shrink progressively until no more additional changed objects are identified.

As described above, the whole procedure was only applied on a single image difference. It was, however, repeated respectively for both image differences and the results were combined, in the sense that an object detected as an outlier in at least one of the statistical tests was considered as “changed” for the whole change detection process.

4. Experimental design

The proposed object-based methodology was tested on the SPOT-HRV images in order to assess its performance using only the NDVI series on one hand (OB-NDVI) and using all of the 9 reflectance bands on the other hand (OB-Reflectance). These results were compared to a robust pixel-based method, i.e., the RGB-NDVI (Sader et al., 2001) and an extension of this technique, the Multispectral Multidate Classification (MMC).

4.1. Object-based change detections

The multivariate segmentation was carried out from the 9 TOA reflectance bands of the SPOT images using equal weights for all bands. The segmentation parameters w_{sp} and w_{cp} of Eq. (2) were equal respectively set at 0.5 and 0.5, as we have no clue about the relative patterns between spectral vs. shape and between compactness vs. smoothness. The h_{sc} was set at 5 to obtain image segmentation with a minimum object size (equal to the Minimum Mapping Unit, the MMU) of 0.5 ha, or 12 pixels of the SPOT-HRV image. This corresponds to a trade-off between the minimum size of change object which could be detected and the number of pixels per object required to compute robust summary statistics.

To compare their respective change detection performances, two separate data sets were prepared: (i) NDVI differences and (ii) TOA reflectance differences. The NDVI differences were computed from the two NDVI paired images, i.e., NDVI95–NDVI92 and NDVI03–NDVI95. For each object obtained from the multivariate segmentation, M and S statistics were extracted from each NDVI difference image, so that for each object i and difference image j , we could define the corresponding vector $\mathbf{X}_{ij} = (M_{ij}, S_{ij})'$. The iterative trimming procedure was applied to each image difference and the results of these 2 analyses were combined. Whereas the confidence level is generally set at 0.99 in statistical tests, a preliminary optimisation of this parameter was completed to maximize the overall accuracy of the change detection algorithm. The appropriate confidence level was thus selected thanks to an optimisation step based on a training set of 1230 objects. For the NDVI data set, the optimised confidence level $1 - \alpha$ was equal to 0.75. This approach will be named hereafter Object-Based method using NDVI (OB-NDVI).

Similarly, the same protocol was applied to the reflectance difference data set (OB-Reflectance) from the two multispectral images differences XS95–XS92 and XS03–XS95, where each image difference includes 3 difference bands, i.e., the NIR, Red and Green. For each object i and difference image j , the corresponding vector is thus $\mathbf{X}_{ij} = (M_{ij1}, M_{ij2}, M_{ij3}, S_{ij1}, S_{ij2}, S_{ij3})'$. The trimming procedure was run separately for each image difference and the results obtained separately for the 2 image differences were combined. The confidence level $1 - \alpha$ equal to 0.99 for OB-Reflectance was selected by an optimisation step (see Section 5.3).

4.2. Pixel-based change detections

Using the 3 NDVI bands of the multivariate SPOT data set, the RGB-NDVI technique of Sader et al. (2001) was applied to produce change maps. The unsupervised ISODATA clustering algorithm (Richards, 1993) produced 45 multi-temporal classes which were interactively labelled in binary format (change vs. no-change) based on the visual interpretation of the color composites without using validation data set.

Similarly, this technique was extended to a more general multispectral multivariate classification (MMC) using the Green,

Red and NIR bands of the three SPOT images, i.e., 9 bands. The unsupervised ISODATA classification also subdivided 45 classes interactively labelled into change or no-change.

4.3. Accuracy assessment

Among the various accuracy assessment methods presented by Biging et al. (1999) and Foody (2002), the change detection error matrix was chosen and computed for each change map. According to Zhan et al. (2002), 4 accuracy indices derived from this error matrix are required to compare these change detection methods. The *overall accuracy* is the proportion of changed and unchanged elements (objects or pixels) that are correctly classified by the method. The *detection accuracy* is the proportion of correctly detected changed elements. The *omission error* is the proportion of omitted changed elements, while the *commission error* is the proportion of falsely detected unchanged elements. κ analysis (Cohen, 1960) uses the overall Kappa and the per-class Kappa statistic, which is a measure of accuracy or agreement based on the difference between the error matrix and chance agreement (Rosenfield & Fitzpatrick-Lins, 1986).

The comparison between different category of change detection techniques requires three types of validation approach: (i) a polygon-wise validation for the object-based method, (ii) a pixel-wise for the pixel-based method and (iii) a polygon-wise for the pixel-based method. First, for a polygon-based mapping output, any pixel-based accuracy assessment would tend to underestimate the map accuracy (Biging et al., 1999). The proposed object-based method was thus evaluated in a polygon-wise way. Each object randomly selected for the accuracy assessment was compared to the corresponding forest parcel of the validation data set. The change label (change or no-change) was compared to the change attribute of the reference data. Given that the selected MMU is 0.5 ha, an object is validated as changed if more than 0.5 ha of its area is covered by a change forest stand of the validation data set. Second, the multivariate classification is a pixel-based change detection method and was evaluated by a pixel-wise assessment. Third, in order to directly compare the two change detection methods, the change maps obtained by multivariate classification were assessed not only pixel-wise but also polygon-wise, following the example of Zhan et al. (2002). For the polygon-wise assessment of the pixel-based method, the change attribute of each polygon was derived from the area of the changed pixels. If this changed area is higher than the MMU defined at 0.5 ha, the polygon is classified as changed.

Two sources of reference data were considered as complementary for the method assessment. The first reference data set was based on the visual interpretation of each one of the 1000 objects randomly selected out of the about 22,000 objects processed by the algorithm. From the false color composite of each date, each of the 1000 objects was interpreted as changed or unchanged. The second reference data set consists of approximately 325 randomly selected objects where forest inventory information was available. Not based on these satellite images, this independent data set strengthened the

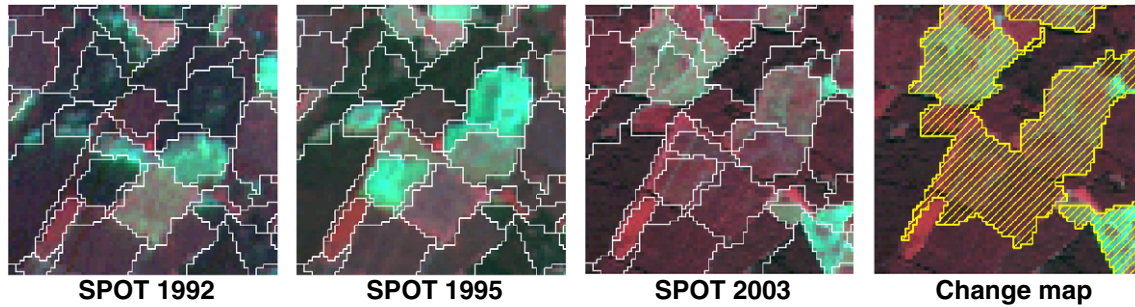


Fig. 3. False color composite subsets (RGB=NIR–Red–Green) of each image of the SPOT time series (1992–1995–2003) overlaid by the multivariate segmentation result. Bright objects are clear-cuts while regions in reddish grey are regenerating areas. The hatched regions on the change map correspond to detected changed objects by the OB-Reflectance method.

accuracy assessment. Because of random selection, changed vs. unchanged samples were not evenly distributed and the proportions of changed objects were equal to 33% for visual interpretation and 20% for forest inventory.

5. Results

Four change maps have been produced based on the 4 change detection techniques, namely RGB-NDVI, OB-NDVI, MMC and OB-Reflectance. From the performance indices assessment, the method comparison has been done separately for each input data, namely the NDVI and the reflectance. Depending of the change detection objectives, the proposed object-based method can be tuned by a preliminary optimisation step, presented for OB-Reflectance in Section 5.3. An example of the OB-Reflectance change map is presented in Fig. 3 beside the corresponding multi-year images.

5.1. Methods comparison using NDVI

Table 1 shows the accuracy assessment results based on four performance indices computed from OB-NDVI and RGB-NDVI change maps using both validation approaches and both reference data set. The overall accuracy of both change maps was similar (about 83%) but the high proportion of unchanged objects made this index less appropriate to evaluate the change detection algorithm. The detection accuracy which is a more informative index to assess the change detection performances

was much higher for OB-NDVI (65%) than for RGB-NDVI (51%). The efficiency of this algorithm was also reported by the omission error (35% vs. 49%) and the commission error (18% vs. 29%). For the polygon-wise validation, the RGB-NDVI detection accuracy was higher whereas the overall accuracy was lower. For the change class, the Kappa statistic was higher for OB-NDVI (0.52) than for RGB-NDVI (0.40), and the overall kappas were respectively 0.61 vs. 0.49. The independent reference data set derived from the forest inventory confirmed these results. The detection accuracy was still higher for the object-based method (66% vs. 49%).

5.2. Methods comparison using reflectance data

Table 2 summarizes the validation results for both change detection methods using all calibrated reflectance channels, i.e., OB-Reflectance and MMC. While the performances of the pixel-based method remained about the same as when using NDVI, the object-based accuracy was improved using reflectances. Indeed, the OB-Reflectance overall accuracy was as high as 93% whatever the validation source. Similarly, the detection accuracy was found superior to 91% for the proposed technique, while omission and commission errors were reduced. The MMC commission errors were low (16%) but can be considered as a logical consequence of the 51% omission errors. The polygon-wise validation of the multivariate classification (MMC) again provided detection accuracy better than the pixel-wise. The increase in commission error was

Table 1

Performance indices for both change detection methods using NDVI, as estimated by two validation approaches, i.e., polygon-wise and pixel-wise, and two sources of reference data, i.e., visual interpretation ($n=1000$) and forest inventory database ($n=325$, between brackets)

Change detection method	OB-NDVI	RGB-NDVI	RGB-NDVI
Validation approach	Polygon-wise	Polygon-wise	Pixel-wise
Detection accuracy (%)	64.6 (66.2)	64.3 (58.8)	50.6 (49.2)
Omission error (%)	35.4 (33.8)	35.7 (41.2)	49.4 (50.8)
Commission error (%)	18.1 (26.2)	39.0 (56.0)	28.6 (32.6)
Overall accuracy (%)	83.7 (88.0)	74.8 (75.7)	82.7 (86.6)
Kappa: change class	0.52 (0.58)	0.45 (0.43)	0.40 (0.41)
Kappa: no-change class	0.73 (0.67)	0.42 (0.29)	0.62 (0.60)
Overall kappa	0.61 (0.62)	0.44 (0.35)	0.49 (0.49)

Table 2

Performance indices for both change detection methods using Reflectances, as estimated by two validation approaches, i.e., polygon-wise and pixel-wise, and two sources of reference data, i.e., visual interpretation ($n=1000$) and forest inventory database ($n=325$, between brackets)

Change detection method	OB-Reflectance	MMC	MMC
Validation technique	Polygon-wise	Polygon-wise	Pixel-wise
Detection accuracy (%)	91.5 (91.2)	54.9 (70.6)	49.4 (62.7)
Omission error (%)	8.5 (8.8)	45.1 (29.4)	50.6 (37.3)
Commission error (%)	13.0 (21.5)	24.7 (32.4)	15.9 (17.8)
Overall accuracy (%)	92.7 (92.9)	79.3 (86.8)	85.1 (90.9)
Kappa: change class	0.87 (0.88)	0.41 (0.62)	0.41 (0.57)
Kappa: no-change class	0.81 (0.73)	0.63 (0.59)	0.79 (0.78)
Overall kappa	0.84 (0.80)	0.50 (0.61)	0.54 (0.66)

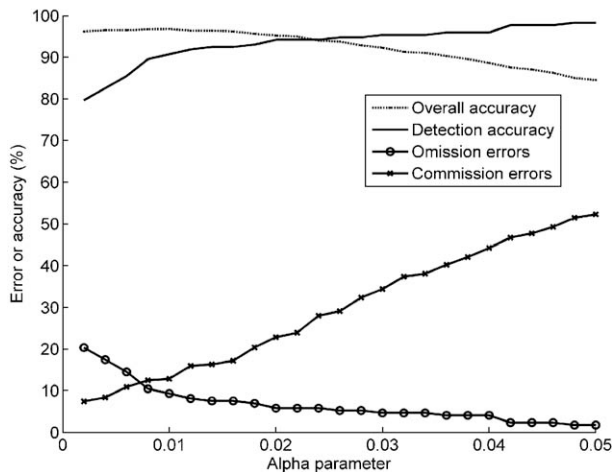


Fig. 4. Evolution of 4 performance indices as a function of the alpha parameter (α) defining the confidence level ($1 - \alpha$) for the OB-Reflectance method.

offset by the decrease in omission error, so the overall accuracy remains about the same. The two per-class κ were similar for the OB-Reflectance (0.87 vs. 0.81) whereas the κ for the change class was lower than the no-change class for MMC (0.41 vs. 0.79). The OB-Reflectance overall kappa was much higher than using the MMC method. The independent reference data set derived from the forest inventory also confirmed these results. The OB-Reflectance detection accuracy was still higher (91% vs. 63%).

5.3. OB-Reflectance optimisation

Due to its statistical design, the object-based method can be optimised according to the purpose of the change detection. Indeed, the alpha parameter (α) in the statistical test defines the confidence level $1 - \alpha$ and can be tuned either to maximize one of the performance indices or to balance both of them. From a subset of 1230 objects (different from the validation set), the four detection performance indices were computed for different α values using the OB-Reflectance (Fig. 4). For $\alpha=0.002$ up to 0.05, the omission error decreased whereas the commission error logically increased. The detection accuracy increased with α , reaching 100% accuracy for $\alpha=0.05$. In this case, the commission errors were high (about 52%) corresponding to many false change alerts. Whereas the overall accuracy was still the same for $\alpha=0.002$ up to 0.02, the detection accuracy variation was about 20%. Using the reflectance, the highest overall accuracy combining both errors was reached for $\alpha=0.01$.

These tuning capabilities allow the user to customize the change detection method with respect to the project objectives. For forest map updating that includes a field visit of the changed areas, the detection accuracy would be maximized so that a high α value, e.g., $\alpha=0.03$, should be preferred. The selection of the confidence level value could be tuned depending of the human resources available for field surveys. In contrast, the maximisation of the overall accuracy of the change detection algorithm should be

preferred for other applications. For example, the forest change for biodiversity or carbon stocks studies can be estimated by this change detection technique using an alpha value (α) below 0.01 to balance omission and commission errors.

6. Discussion

As outlined above, the proposed OB-Reflectance method combines the advantages and strengths of three methodological aspects; i.e., image segmentation, image differencing and statistical testing.

Through the object-based approach, the initial multivariate segmentation process insures the quality of the multispectral data to be submitted to iterative trimming. Indeed, the object delineation combined the spectral, temporal and spatial information to create consistent units of interest for statistical analysis. The segmentation is also less sensitive to misregistration errors than traditional pixel-based analysis methods (Mäkelä & Pekkarinen, 2001) and reduces the change detection processing time given that there are much fewer objects than pixels. Moreover, the object boundaries derived directly from the satellite images are more consistent than using GIS data which sometimes have non-reconcilable boundaries when overlaid on these images. Based on these objects, the subsequent statistical analyses are thus more robust and the change detection performances are increased. It is worth noting that the objects defined by the multivariate segmentation do not necessarily correspond to real stands on the field. In particular, the selection of only one segmentation scale for the analysis constrains the object size and may sometimes prevent the delineation of either very large stands or spatially limited changes. However, this multivariate segmentation was found to be better than a combination of independent segmentations on each image that easily leads to over-segmentation with sliver polygons.

The multivariate image comparison was performed using image differencing. Many change detection studies have been based on the single vegetation index NDVI to reduce the differences in illumination and topographic effects (Hayes & Sader, 2001; Lyon et al., 1998; Wilson & Sader, 2002). While reflectance differencing is a well-known technique for change detection, the comparison of these reflectance differences by way of iterative trimming makes this approach very robust, even without accurate radiometric calibration. Moreover, due to the sun synchronous character of the SPOT satellite, topographic effects are supposed to be constants between images. It should be noted, however, that, after the cloud coverage screening, the method assumes that atmospheric effects are homogeneous over the whole study area. Heterogeneous atmospheric effects may require a preliminary stratification of the region or indeed, corrections of these effects (Song et al., 2001).

The use of a statistical procedure makes the method scene-independent. The multivariate reflectance is considered as very homogeneous for unchanged objects which are very numerous compared to changed ones. The detection of these rare objects

having abnormal multivariate reflectance is done thanks to the combination of both statistics, M and S , from the object multivariate signature. Whereas only the object mean (M) is computed in several object-based methods (Saksa et al., 2003; Wulder et al., 2004), the addition of the object standard deviation (S) was found to be very efficient. Moreover, the comparison of algorithm performance in this study illustrated that the most relevant input data for change detection are the whole set of spectral channels (NIR, Red and Green) rather than a combination of these channels in the NDVI. Changed objects are better identified when the spectral band number increases as a land cover change could affect only one spectral band.

The change detection results of the proposed method were found higher than many studies reported in the literature. Indeed, the OB-Reflectance method has achieved an overall accuracy of 93% and an overall kappa of 0.84. The particular unsupervised multivariate classification developed by Häme et al. (1998) was found less efficient for change extraction (respectively 66% and 0.21). Hayes and Sader (2001) have assessed three different methods using the same performance indices: PCA method (74% and 0.69), NDVI differencing (82% and 0.79) and RGB-NDVI (85% and 0.83). Using change vector analysis, Lunetta et al. (2004) achieved quite good performances (86% and 0.55). High results (92% and 0.87) were obtained by Rogan et al. (2003) using classification trees which can be considered as scene-dependent. For the RGB-NDVI method, the performance achieved by this study corresponds to those from the literature (Hayes & Sader, 2001). They were even higher (83% and 0.49) than the 64% and 0.29 achieved by Wilson and Sader (2002, Table 8) using 3 NDVI bands.

The comparison between object-based and pixel-based is a difficult task. Using both polygon-wise and pixel-wise validations, the analysis of our performance showed two particular trends. First, the polygon-wise validation of the multivariate classification provides lower overall accuracy than the pixel-wise. In the polygon-wise validation, objects with pixels classified as 'changed' covering an area larger than the Minimum Mapping Unit (MMU) are considered as changed. So, omission errors are reduced whereas commission errors are more numerous, thus reducing the overall accuracy. This polygon-wise validation is thus not suitable for accuracy assessment of a pixel-based method except for the sake of comparison between pixel-based and polygon-based method. Secondly, the overall accuracy is slightly higher using forest inventory as reference whereas commission errors are more frequent for all detection methods. The increase of false change alerts can be explained by the larger proportion of unchanged forest stands in the forest inventory.

This approach has proved to be very efficient for forest change extraction and offers the advantage of being an automated procedure. Indeed, no predefined threshold for reflectance difference channels was required in this analysis. There were only two parameters to be set by the user: (i) the scale parameter h_{scale} and (ii) the confidence level $1 - \alpha$ of the statistical test. The first was based on the MMU expected from the change analysis. The second relied on the proportion of

changed vs. unchanged objects. Although the default parameter settings already provide satisfactory results, the fine-tuning capabilities offered by the method allow the user to optimise it with respect to the considered application. In our study, this level of confidence was tuned at 0.99 for the OB-Reflectance by an optimisation procedure on overall accuracy.

Whereas most of the change detection studies cope with change extraction and change labelling analyses, this study was focused mainly on the extraction of change regions. From change detection results, the visual interpretation can be focused on the rare changed objects to determine the type of land cover change. Moreover, the performance of extraction can be assessed independently of the change labelling. It is important to mention that all types of forest changes, e.g., clear-cutting, reforestation, etc., were detected using the same processing algorithm and that no very precise measurement of their size or shapes have been done.

7. Conclusions

The object-based change detection method proposed here proved to be very efficient to identify forest land cover changes in both deciduous and coniferous stands. A detection accuracy higher than 90% and an overall kappa higher than 0.80 were achieved using a SPOT multivariate data set covering a 10-years time span. This technique can be considered scene-independent in the sense that no predefined threshold for reflectance difference channels of the multivariate image was required. Moreover, the fine-tuning capabilities of a single algorithm parameter allow the user to customize the change detection technique according to its specific objectives. The change detection results achieved by the object-based method were higher than pixel-based methods, regardless of the validation data source.

Given its scene-independent property and its sound statistical formulation, the proposed object-based method can be easily extended to other kinds of data, other regions, or even for monitoring surface changes in non-forested areas. Other experiments using various sensors in various environments are needed in order to extend this very promising method for land surface monitoring and map updating.

Whereas this study was focused mainly on the extraction of change regions without distinction about the nature of these changes, it could be very useful to address the problem of change type classification inside the procedure itself. Further theoretical developments are still needed for this. Improving the exact delineation of detected changed stands is another aspect that could also be helpful to develop in the future, especially if the aim is to obtain quantitative assessments about the change area.

Acknowledgements

This research has been funded by the Belgian National Fund for Scientific Research (FNRS) by the way of an FRIA grant. The satellite data have been made available by the Belgian Science Policy Office (BSPO). The authors wish to thank the

“Division of Nature and Forest” (DNF) for providing them with the forest inventory GIS data and the “National Geographic Institute” (NGI) for the Top10v-GIS data used for the field survey. The authors thank also the reviewers for their constructive comments and remarks.

References

- Asner, G. P., Keller, M., Pereira, R., & Zweede, J. C. (2002). Remote sensing of selective logging in Amazonia—Assessing limitations based on detailed field observations, Landsat ETM+, and textural analysis. *Remote Sensing of Environment*, *80*, 483–496.
- Atkinson, P. M., & Lewis, P. (2000). Geostatistical classification for remote sensing: An introduction. *Computers and Geosciences*, *26*, 361–371.
- Baatz, M., & Schäpe, A. (2000). Multiresolution segmentation: An optimization approach for high quality multiscale image segmentation. In J. Strbl, & T. Blaschke (Eds.), *Angewandte Geographische Informationsverarbeitung* (pp. 12–23). Heidelberg: Wichmann.
- Bickel, P. J. (1965). On some robust estimates of location. *The Annals of Mathematical Statistics*, *36*(3), 847–858.
- Biging, G. S., Colby, D. R., & Congalton, R. G. (1999). Sampling systems for change detection accuracy assessment. In R. S. Lunetta, & C. D. Elvidge (Eds.), *Remote sensing change detection: Environmental monitoring methods and applications* (pp. 281–308). Chelsea: Ann Arbor Press.
- Bruzzone, L., & Prieto, D. F. (2000). Automatic analysis of the difference image for unsupervised change detection. *IEEE Transactions on Geoscience and Remote Sensing*, *38*, 1171–1182.
- Büttner, G., Feranec, F., and Jaffrain, G. (2002). *Corine land cover update 2000*. Technical report. Copenhagen: European Environment Agency.
- Cohen, J. (1960). A coefficient of agreement for nominal scales. *Educational and Psychological Measurement*, *20*, 37–46.
- Coppin, P. R., & Bauer, M. E. (1994). Processing of multitemporal Landsat TM imagery to optimize extraction of forest cover change features. *IEEE Transactions on Geoscience and Remote Sensing*, *32*, 918–927.
- Coppin, P. R., & Bauer, M. E. (1995). The potential contribution of pixel-based canopy change information to stand-based forest management in the northern U.S. *Journal of Environmental Management*, *44*, 69–82.
- Coppin, P. R., & Bauer, M. E. (1996). Digital change detection in forest ecosystems with remote sensing imagery. *Remote Sensing Reviews*, *13*, 207–234.
- de Wasseige, C., & Defourny, P. (2004). Remote sensing of selective logging impact for tropical forest management. *Forest Ecology and Management*, *188*, 161–173.
- FAO (2001). Global forest resources assessment 2000. Report No. FAO Forestry Paper 140 (Food and Agriculture Organization of the United Nations, Rome).
- Flanders, D., Hall-Beyer, M., & Pereverzoff, J. (2003). Preliminary evaluation of eCognition object-based software for cut block delineation and feature extraction. *Canadian Journal of Remote Sensing*, *29*(4), 441–452.
- Foody, G. M. (2002). Status of land cover classification accuracy assessment. *Remote Sensing of Environment*, *80*, 185–201.
- Foody, G. M. (2003). Remote sensing of tropical forest environments: Towards the monitoring of environmental resources for sustainable development. *International Journal of Remote Sensing*, *24*, 4035–4046.
- Fung, T., & LeDrew, E. (1988). The determination of optimal threshold levels for change detection using various accuracy indices. *Photogrammetric Engineering and Remote Sensing*, *54*, 1449–1454.
- Hall, R. J., Crown, P. H., & Titus, S. J. (1984). Change detection methodology for aspen defoliation with Landsat MSS digital data. *Canadian Journal of Remote Sensing*, *10*, 135–142.
- Häme, T. (1991). Spectral interpretation of changes in forest using satellite scanner images. *Acta forestalia fennica*, vol. 222. Helsinki: The Society of Forest in Finland – The Finnish Forest Research Institute.
- Häme, T., Heiler, I., & Miguel-Ayanz, J. (1998). An unsupervised change detection and recognition system for forestry. *International Journal of Remote Sensing*, *19*, 1079–1099.
- Hayes, D. J., & Sader, S. A. (2001). Comparison of change-detection techniques for monitoring tropical forest clearing and vegetation regrowth in a time series. *Photogrammetric Engineering and Remote Sensing*, *67*, 1067–1075.
- Heikkonen, J., & Varjo, J. (2004). Forest change detection applying Landsat Thematic Mapper difference features: A comparison of different classifiers in boreal forest conditions. *Forest Science*, *50*, 579–588.
- Hoaglin, D. C., Mosteller, F., & Tukey, J. W. (1983). *Understanding robust and exploratory data analysis*. New York: Wiley.
- Huber, P. J. (1972). The 1972 Wald lecture robust statistics: A review. *The Annals of Mathematical Statistics*, *43*(4), 1041–1067.
- Jin, S. M., & Sader, S. A. (2005). Comparison of time series tasseled cap wetness and the normalized difference moisture index in detecting forest disturbances. *Remote Sensing of Environment*, *94*, 364–372.
- Kayitakire, F., Giot, P., & Defourny, P. (2002). Automated delineation of the forest stands using digital color orthophotos: Case study in Belgium. *Canadian Journal of Remote Sensing*, *28*, 629–640.
- Kotz, S., Johnson, N. L., & Read, C. (1988). *Encyclopedia of statistical sciences*. New York: Wiley.
- Lee, S. (1995). A trimmed mean of location of an AR(∞) stationary process. *Journal of Statistical Planning and Inference*, *48*, 131–140.
- Le Hégarat-Masclé, S., & Seltz, R. (2004). Automatic change detection by evidential fusion of change indices. *Remote Sensing of Environment*, *91*, 390–404.
- Li, X., & Yeh, A. G. O. (1998). Principal component analysis of stacked multi-temporal images for the monitoring of rapid urban expansion in the Pearl River Delta. *International Journal of Remote Sensing*, *19*, 1501–1518.
- Liang, S., Fallah-Adl, H., Kalluri, S., Jaja, J., Kauffman, Y. J., & Townshend, J. R. G. (1997). An operational atmospheric correction algorithm for Landsat Thematic Mapper imagery over the land. *Journal of Geophysical Research*, *102*, 173–186.
- Lillesand, T. M., & Kiefer, R. W. (2000). *Remote sensing and image interpretation* (4th ed.). New York: Wiley.
- Lobo, A. (1997). Image segmentation and discriminant analysis for the identification of land cover units in ecology. *IEEE Transactions on Geoscience and Remote Sensing*, *35*, 1136–1145.
- Lu, D., Mausel, P., Brondizio, E., & Moran, E. (2004). Change detection techniques. *International Journal of Remote Sensing*, *25*, 2365–2407.
- Lunetta, R. S., Johnson, D. M., Lyon, J. G., & Crotwell, J. (2004). Impacts of imagery temporal frequency on land-cover change detection monitoring. *Remote Sensing of Environment*, *89*, 444–454.
- Lyon, J., Yuan, D., Lunetta, R., & Elvidge, C. (1998). A change detection experiment using vegetation indices. *Photogrammetric Engineering and Remote Sensing*, *64*, 143–150.
- Macomber, S. A., & Woodcock, C. E. (1994). Mapping and monitoring conifer mortality using remote-sensing in the lake Tahoe basin. *Remote Sensing of Environment*, *50*, 255–266.
- Mäkelä, H., & Pekkarinen, A. (2001). Estimation of timber volume at the sample plot level by means of image segmentation and Landsat TM imagery. *Remote Sensing of Environment*, *77*, 66–75.
- Richards, J. A. (1993). *Remote sensing digital image analysis. An introduction* (2nd ed.). Berlin: Springer-Verlag, 340 pp.
- Ridd, M. K., & Liu, J. J. (1998). A comparison of four algorithms for change detection in an urban environment. *Remote Sensing of Environment*, *63*, 95–100.
- Rogan, J., & Chen, D. M. (2004). Remote sensing technology for mapping and monitoring land-cover and land-use change. *Progress in Planning*, *61*, 301–325.
- Rogan, J., Miller, J., Stow, D., Franklin, J., Levien, L., & Fischer, C. (2003). Land-cover change monitoring with classification trees using Landsat TM and ancillary data. *Photogrammetric Engineering and Remote Sensing*, *69*, 793–804.
- Rosenfield, G. H., & Fitzpatrick-Lins, A. (1986). A coefficient of agreement as a measure of thematic classification accuracy. *Photogrammetric Engineering and Remote Sensing*, *52*, 223–227.
- Sader, S. A., Hayes, D. J., Hepinstall, J. A., Coan, M., & Soza, C. (2001). Forest change monitoring of a remote biosphere reserve. *International Journal of Remote Sensing*, *22*(10), 1937–1950.

- Saksa, T., Uuttera, J., Kolstrom, T., Lehtikoinen, M., Pekkarinen, A., & Sarvi, V. (2003). Clear-cut detection in boreal forest aided by remote sensing. *Scandinavian Journal of Forest Research*, 18, 537–546.
- Saura, S. (2002). Effects of minimum mapping unit on land cover data spatial configuration and composition. *International Journal of Remote Sensing*, 23, 4853–4880.
- Silapaswan, C. S., Verbyla, D. L., & McGuire, A. D. (2001). Land cover change on the Seward Peninsula: The use of remote sensing to evaluate the potential influences of climate warming on historical vegetation dynamics. *Canadian Journal of Remote Sensing*, 27, 542–554.
- Song, C., Woodcock, C. E., Seto, K. C., Lenney, M. P., & Macomber, S. A. (2001). Classification and change detection using Landsat TM data: When and how to correct atmospheric effects? *Remote Sensing of Environment*, 75, 230–244.
- Sunar, F. (1998). An analysis of changes in a multi-date data set: a case study in the Ikitelli area, Istanbul, Turkey. *International Journal of Remote Sensing*, 19, 225–235.
- Townshend, J. R. G., Huang, C., Kalluri, S. N. V., DeFries, R. S., Liang, S., & Yang, K. (2000). Beware of per-pixel characterization of land cover. *International Journal of Remote Sensing*, 21, 839–843.
- Varjo, J. (1996). Controlling continuously updated forest data by satellite remote sensing. *International Journal of Remote Sensing*, 17, 43–67.
- Walter, V. (2004). Object-based classification of remote sensing data for change detection. *ISPRS Journal of Photogrammetry and Remote Sensing*, 58, 225–238.
- Wilson, E. H., & Sader, S. A. (2002). Detection of forest harvest type using multiple dates of Landsat TM imagery. *Remote Sensing of Environment*, 80, 385–396.
- Wulder, A. A., Skakun, R. S., Kurz, W. A., & White, J. C. (2004). Estimating time since forest harvest using segmented Landsat ETM+ imagery. *Remote Sensing of Environment*, 93, 179–187.
- Zhan, Q., Wang, J., Peng, X., Gong, P., & Shi, P. (2002). Urban built-up land change detection with road density and spectral information from multi-temporal Landsat TM data. *International Journal of Remote Sensing*, 23, 3057–3078.